

Rhodium(III)-Catalyzed Arene and Alkene C–H Bond Functionalization Leading to Indoles and Pyrroles

David R. Stuart,^{*,†} Pamela Alsabeh,[‡] Michelle Kuhn, and Keith Fagnou[§]Centre for Catalysis Research and Innovation, Department of Chemistry, University of Ottawa,
10 Marie Curie, Ottawa, (Canada) K1N 6N5

Received September 13, 2010; E-mail: dstuart@fas.harvard.edu

Abstract: Recently, the rhodium(III)-complex $[\text{Cp}^*\text{RhCl}_2]_2$ **1** has provided exciting opportunities for the efficient synthesis of aromatic heterocycles based on a rhodium-catalyzed C–H bond functionalization event. In the present report, the use of complexes **1** and its dicationic analogue $[\text{Cp}^*\text{Rh}(\text{MeCN})_3][\text{SbF}_6]_2$ **2** have been employed in the formation of indoles via the oxidative annulation of acetanilides with internal alkynes. The optimized reaction conditions allow for molecular oxygen to be used as the terminal oxidant in this process, and the reaction may be carried out under mild temperatures (60 °C). These conditions have resulted in an expanded compatibility of the reaction to include a range of new internal alkynes bearing synthetically useful functional groups in moderate to excellent yields. The applicability of the method is exemplified in an efficient synthesis of paullone **3**, a tetracyclic indole derivative with established biological activity. A mechanistic investigation of the reaction, employing deuterium labeling experiments and kinetic analysis, has provided insight into issues of reactivity for both coupling partners as well as aided in the development of conditions for improved regioselectivity with respect to meta-substituted acetanilides. This reaction class has also been extended to include the synthesis of pyrroles. Catalyst **2** efficiently couples substituted enamides with internal alkynes at room temperature to form trisubstituted pyrroles in good to excellent yields. The high functional group compatibility of this reaction enables the elaboration of the pyrrole products into a variety of differentially substituted pyrroles.

Introduction

Indoles and pyrroles represent two of the most abundant heterocycles in nature. As constituents of essential amino acids, embedded in structurally complex biologically active natural products,¹ and possessing desirable properties to materials scientists,² the means for their construction have captivated chemists for over a century (Figure 1).³ Additionally, owing to the prevalence of these heterocycles in known pharmaceuticals, they have been termed a “privileged motif” in medicinal chemistry (Figure 1).⁴ For these reasons, many advances have been made in the synthesis of aromatic heterocycles in recent decades, with transition metal-catalyzed reactions taking a

prominent role.^{5,6} The Larock indole synthesis is paramount among the latter, setting the state-of-the-art for transition metal-catalyzed *intermolecular* approaches toward indoles,^{5d,g,7} and analogous reactions have recently been developed for the synthesis of pyrroles^{6c} and other heterocycles.^{5a} However, these approaches necessitate substrate preactivation in the form of aryl and alkenyl halides, adding to the overall time and cost of a synthetic sequence (Scheme 1, eq 1). More recently, the synthesis of aromatic heterocycles has shifted to include approaches predicated upon a C–H bond functionalization event

[†] Current address: Department of Chemistry & Chemical Biology, Harvard University, Cambridge, MA 02138.

[‡] Current address: Department of Chemistry, Dalhousie University, Halifax, Nova Scotia, (Canada) B3H 4J3.

[§] Deceased, November 11, 2009.

(1) (a) A Beilstein search for indoles with biological activity yielded >45 000 results. (b) Richter, J. M.; Ishihara, Y.; Masuda, T.; Whitefield, B. W.; Llamas, T.; Pohjakallio, A.; Baran, P. S. *J. Am. Chem. Soc.* **2008**, *130*, 17938, and references therein. (c) Fürstner, A. *Angew. Chem., Int. Ed.* **2003**, *43*, 3582.

(2) (a) Yoon, Z. S.; Kwon, J. H.; Yoon, M.-C.; Koh, M. K.; Noh, S. B.; Sessler, J. L.; Lee, J. T.; Seidel, D.; Aguilar, A.; Shimizu, S.; Suzuki, M.; Osuka, A.; Kim, D. *J. Am. Chem. Soc.* **2006**, *128*, 14128. (b) Lee, J.-S.; Kang, N.-Y.; Kim, Y. K.; Samanta, A.; Feng, S.; Kim, H. K.; Vendrell, M.; Park, J. H.; Chang, Y.-T. *J. Am. Chem. Soc.* **2009**, *131*, 10077.

(3) Gilchrist, T. L. *J. Chem. Soc., Perkin Trans. 1* **1999**, 2849.

(4) de Sá Alves, F. R.; Barreiro, E. J.; Fraga, C. A. M. *Mini-Rev. Med. Chem.* **2009**, *9*, 782.

(5) For a review on transition metal-catalyzed indole synthesis, see: (a) Zeni, G.; Larock, R. C. *Chem. Rev.* **2006**, *106*, 4644. For selected individual accounts, see: (b) Tida, H.; Yuasa, Y.; Kibayashi, C. *J. Org. Chem.* **1980**, *45*, 2938. (c) Sakamoto, T.; Nagano, T.; Kondo, Y.; Yamanaka, H. *Synthesis* **1990**, 215. (d) Larock, R. C.; Yum, E. K. *J. Am. Chem. Soc.* **1991**, *113*, 6689. (e) Koerber-Ple, K.; Massiot, G. *Synlett* **1994**, 759. (f) Chen, C. Y.; Lieberman, D. R.; Larsen, R. D.; Verhoeven, T. R.; Reider, P. J. *J. Org. Chem.* **1997**, *62*, 2676. (g) Larock, R. C.; Yum, E. K.; Refvik, M. D. *J. Org. Chem.* **1998**, *63*, 7652. (h) Yamazaki, K.; Nakamura, Y.; Kondo, Y. *J. Org. Chem.* **2003**, *68*, 6011. (i) Watanabe, T.; Arai, S.; Nishida, A. *Synlett* **2004**, 907. (j) Nazare, M.; Schneider, C.; Lindenschmidt, A.; Will, D. W. *Angew. Chem., Int. Ed.* **2004**, *43*, 4526. (k) Jia, Y.; Zhu, J. *J. Org. Chem.* **2006**, *71*, 7826. (l) Leogane, O.; Lebel, H. *Angew. Chem., Int. Ed.* **2008**, *47*, 350.

(6) For selected examples of transition metal-catalyzed pyrrole synthesis, see: (a) Dhawan, R.; Arndtsen, B. A. *J. Am. Chem. Soc.* **2004**, *126*, 468. (b) Lu, Y.; Arndtsen, B. A. *Angew. Chem., Int. Ed.* **2008**, *47*, 5430. (c) Crawley, M. L.; Goljer, I.; Jenkins, D. J.; Mehlmann, J. F.; Nogle, L.; Dooley, R.; Mahaney, P. E. *Org. Lett.* **2006**, *8*, 5837. (d) Kel'in, A. V.; Sromek, A. W.; Gevorgyan, V. *J. Am. Chem. Soc.* **2001**, *123*, 2075. (e) Gabriele, B.; Salerno, G.; Fazio, A. *J. Org. Chem.* **2003**, *68*, 7853.

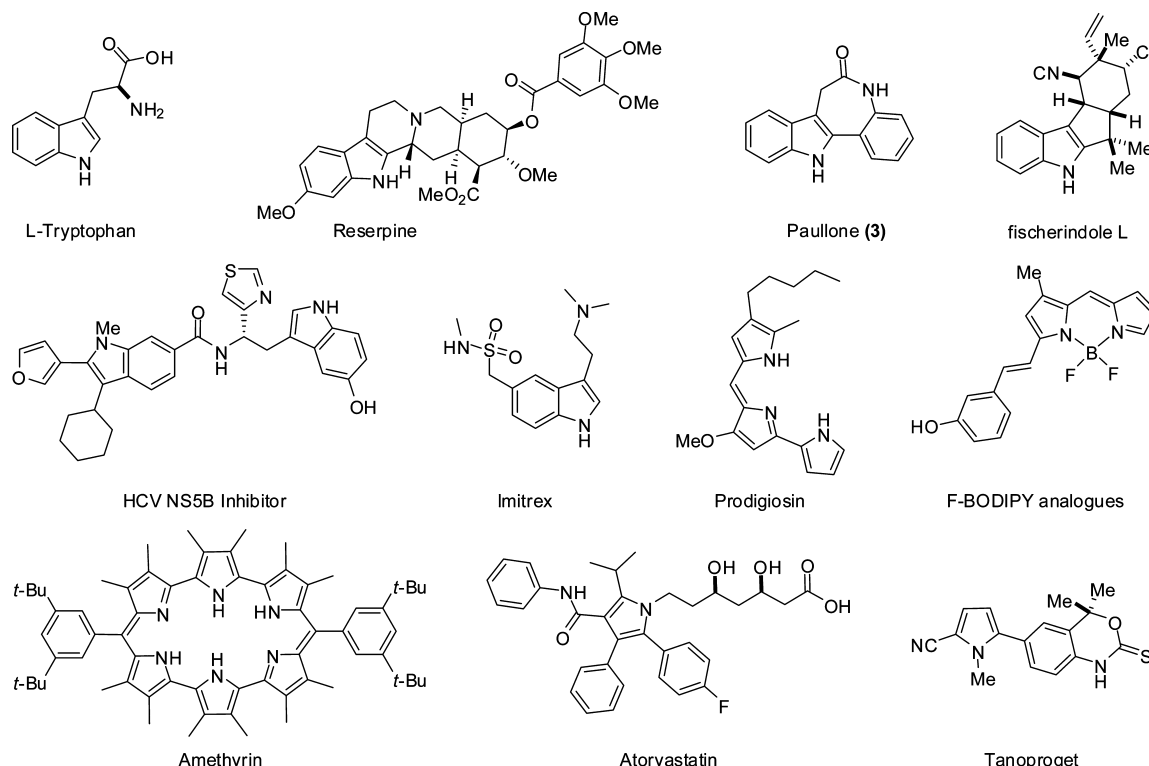


Figure 1. Representative important indoles and pyrroles.

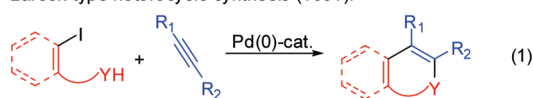
which represents an inherently more efficient and atom economical approach (Scheme 1, eq 2).⁸ Within these methods, palladium, copper, and rhodium catalysts have been employed in the synthesis of isocoumarins,⁹ indoles,¹⁰ indolines,¹¹ pyr-

roles,¹² isoquinolines,¹³ and isoquinolones and pyridones¹⁴ among other heterocycles.¹⁵ Rhodium(III)-catalysts have been particularly useful in these transformations, in which rhodium is often introduced as the $[\text{Cp}^*\text{RhCl}_2]_2$ 1 catalyst precursor.^{9,10b,12–15}

Our group has successfully implemented this approach, employing rhodium(III)-catalysts, in the preparation of a number of heterocycles,^{10b,13b,14a} as well as in the hydroarylation of unactivated internal alkynes.¹⁶ However, in our previous indole synthesis (eq 3), and in many other cases within this reaction

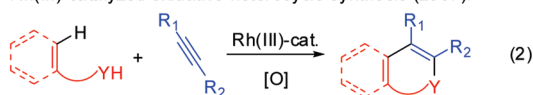
Scheme 1. Recent Transition Metal-Catalyzed Approaches to Aromatic Heterocycles

Larock-type heterocycle synthesis (1991):

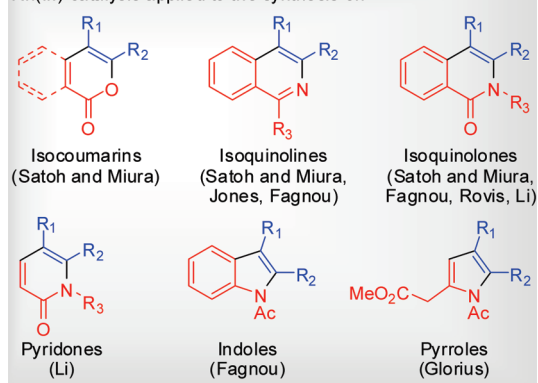


Y = O, C(CH₃)₂O, CO₂Me (H not present), NR

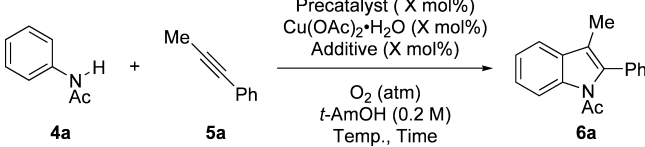
Rh(III)-catalyzed oxidative heterocycle synthesis (2007):



Rh(III)-catalysis applied to the synthesis of:



- (7) For representative applications in medicinal chemistry, see: (a) Lanter, J. C.; Fiordeliso, J. J.; Alford, V. C.; Zhang, X.; Wells, K. M.; Russell, R. K.; Allan, G. F.; Lai, M.-T.; Linton, O. L.; Lundeen, S.; Sui, Z. *Bioorg. Med. Chem. Lett.* **2007**, *17*, 2545. (b) Watterson, S. H.; Murali Dhar, T. G.; Ballentine, S. K.; Shen, Z.; Barrish, J. C.; Cheney, D.; Fleener, C. A.; Rouleau, K. A.; Townsend, R.; Hollenbaugh, D. L.; Iwanowicz, E. J. *Bioorg. Med. Chem. Lett.* **2003**, *13*, 1273. (c) Curtis, N. R.; Kulagowski, J. J.; Leeson, P. D.; Ridgill, M. P.; Emms, F.; Freedman, S. B.; Patel, S.; Patel, S. *Bioorg. Med. Chem. Lett.* **1999**, *9*, 585. (d) Ujjainwalla, F.; Walsh, T. F. *Tetrahedron Lett.* **2001**, *41*, 6441. For recent representative examples of the Larock indole synthesis in total synthesis, see: (e) Newhouse, T.; Lewis, C. A.; Baran, P. S. *J. Am. Chem. Soc.* **2009**, *131*, 6360. (f) Newhouse, T.; Baran, P. S. *J. Am. Chem. Soc.* **2008**, *130*, 10886. (g) Newhouse, T.; Lewis, C. A.; Eastman, K. J.; Baran, P. S. *J. Am. Chem. Soc.* **2010**, *132*, 7119. (h) Garfunkle, J.; Kimball, F. S.; Trzuppek, J. D.; Takizawa, S.; Shimamura, H.; Tomishima, M.; Boger, D. L. *J. Am. Chem. Soc.* **2009**, *131*, 16036.
- (8) For a recent and comprehensive review of rhodium(III)-catalyzed formation of heterocycles via annulative processes with internal alkynes, see: Sato, T.; Miura, M. *Chem.-Eur. J.* **2010**, *16*, 11212.
- (9) (a) Ueura, K.; Sato, T.; Miura, M. *Org. Lett.* **2007**, *9*, 1407. (b) Ueura, K.; Sato, T.; Miura, M. *J. Org. Chem.* **2007**, *72*, 5362.
- (10) (a) Wurtz, S.; Rakshit, S.; Neumann, J. J.; Droge, T.; Glorius, F. *Angew. Chem., Int. Ed.* **2008**, *47*, 7230. (b) Stuart, D. R.; Bertrand-Laperle, M.; Burgess, K. M. N.; Fagnou, K. *J. Am. Chem. Soc.* **2008**, *130*, 16474. (c) Shi, Z.; Zhang, C.; Li, S.; Pan, D.; Ding, S.; Cui, Y.; Jiao, N. *Angew. Chem., Int. Ed.* **2009**, *48*, 4572. (d) Bernini, R.; Fabrizi, G.; Sferazza, A.; Cacchi, S. *Angew. Chem., Int. Ed.* **2009**, *48*, 8078. (e) Tan, Y.; Hartwig, J. F. *J. Am. Chem. Soc.* **2010**, *132*, 3676. (f) Chen, J.; Song, G.; Pan, C.-L.; Li, X. *Org. Lett.* **2010**, *12*, 5426.

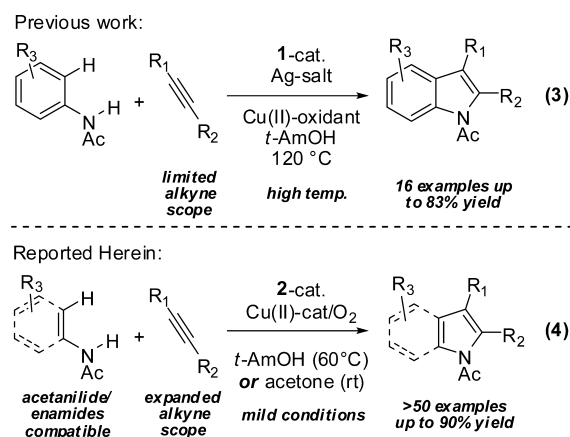
Table 1. Optimization of Second-Generation Conditions


entry	precatalyst (mol %)	additive (mol %)	Cu(OAc) ₂ (mol %)	temp	time (h)	¹ H NMR yield (6a) ^c
1	[Cp*RhCl ₂] ₂ (2.5)	AgSbF ₆ (10)	210 ^b	120 °C	1	86(79)
2	[Cp*RhCl ₂] ₂ (2.5)	AgSbF ₆ (10)	210 ^b	60 °C	6	92(90)
3	[Cp*RhCl ₂] ₂ (2.5)	AgSbF ₆ (10)	10	60 °C	6	55
4	[Cp*RhCl ₂] ₂ (2.5)	AgSbF ₆ (10)	10	60 °C	22	68
5	[Cp*RhCl ₂] ₂ (2.5)	AgSbF ₆ (10)	20	60 °C	22	81
6	[Cp*Rh(MeCN) ₃][SbF ₆] ₂ (5)	—	20	60 °C	22	93(90)
7	[Cp*Rh(MeCN) ₃][SbF ₆] ₂ (5)	—	20	21 °C	30	9 ^d
8	[Cp*Rh(MeCN) ₃][SbF ₆] ₂ (5)	—	20	21 °C	96	12 ^d
9	[Cp*Rh(MeCN) ₃][SbF ₆] ₂ (5)	—	20	21 °C	96	95 ^{d,e}

^a Conditions: **4a** (1 equiv 0.2 M), **5a** (1.1 equiv), precatalyst **1** or **2**, additive (if applicable), Cu(OAc)₂·H₂O, O₂ balloon (if applicable), *t*-AmOH, temperature, specified time. ^b No balloon of O₂ used. ^c NMR yield vs trimethoxybenzene as internal standard; isolated yields in parentheses. ^d GCMS yield vs trimethoxybenzene as internal standard. ^e Reaction performed in acetone.

class, high temperatures (>100 °C) and stoichiometric amounts of a metal oxidant¹⁷ (2 equiv of Cu(OAc)₂) are employed. Additionally, many of these reactions have so far displayed limited compatibility with respect to the alkyne coupling partner.¹⁸ Symmetrical and unsymmetrical dialkyl alkynes are noticeably absent from many recently reported annulations,^{10f,12,14a,b,d,e,15a,c} and, when present, typically provide diminished yields of the desired product in comparison to other alkynes.^{10b,13c,14c,15b} Unsymmetrical dialkyl alkynes are also complicated by low ratios of often inseparable regioisomers.^{10b,14c} Given the recent developments for the synthesis of heterocycles catalyzed by **1**, a detailed mechanistic understanding of this class of reaction will only aid in the further expansion of existing methods and pave the way for future endeavors. In the context of heterocycle synthesis,^{13a} Jones has carried out an elegant mechanistic study on the cyclorhodation of benzylamines with

stoichiometric amounts of **1**.¹⁹ However, a complete mechanistic study of catalytic oxidative annulation reactions utilizing **1** (or related analogues) has yet to be reported and prompted our interest in a broader understanding of the reaction.



In this account, we report our findings in the development of general and mild conditions for the oxidative annulation of acetanilides with internal alkynes catalyzed by the rhodium(III)-complexes **1** and [Cp*Rh(MeCN)₃][SbF₆]₂ **2**. The mild conditions support the use of molecular oxygen as the terminal oxidant and are compatible with a more diverse set of internal alkynes than previously reported (eq 4). The synthetic utility of this transformation is further highlighted by an expedient synthesis of paullone **3**, the parent compound of a family of compounds with known biological activity. Additionally, we have undertaken a mechanistic evaluation of the reaction based on isotope labeling experiments and kinetic analysis. The resulting information has provided answers to some of the issues of regioselectivity for the acetanilide metalation and alkyne insertion steps and guided our development of conditions for improved regioselectivity of meta-substituted acetanilides. Finally, the method is extended to include the room temperature preparation of pyrroles, and the utility of the method is illustrated by the

- (11) Houlden, C. E.; Bailey, C. D.; Ford, J. G.; Gagné, M. R.; Lloyd-Jones, G. C.; Booker-Milburn, K. I. *J. Am. Chem. Soc.* **2008**, *130*, 10066.
- (12) During the preparation of this manuscript, a conceptually interesting approach employing allylic, and one example of vinylic, C–H bond functionalization in the formation of pyrroles was reported; see: Rakshit, S.; Patureau, F. W.; Glorius, F. *J. Am. Chem. Soc.* **2010**, *132*, 9585.
- (13) For an example of stoichiometric [Cp*RhCl₂]₂-mediated isoquinoline salt formation, see: (a) Li, L.; Brennessel, W. W.; Jones, W. D. *J. Am. Chem. Soc.* **2008**, *130*, 12414. For examples of isoquinoline synthesis employing catalytic **1** and **2**, see: (b) Guimond, N.; Fagnou, K. *J. Am. Chem. Soc.* **2009**, *131*, 12050. (c) Fukutani, T.; Umeda, N.; Hirano, K.; Satoh, T.; Miura, M. *Chem. Commun.* **2009**, 5141.
- (14) (a) Guimond, N.; Gouliaras, C.; Fagnou, K. *J. Am. Chem. Soc.* **2010**, *132*, 6908. (b) Mochida, S.; Umeda, N.; Hirano, K.; Satoh, T.; Miura, M. *Chem. Lett.* **2010**, 39, 744. (c) Hyster, T. K.; Rovis, T. *J. Am. Chem. Soc.* **2010**, *132*, 10565. (d) Song, G.; Chen, D.; Pan, C.-L.; Crabtree, R. H.; Li, X. *J. Org. Chem.* **2010**, *75*, 7487. (e) Su, Y.; Zhao, M.; Han, K.; Song, G.; Li, X. *Org. Lett.* **2010**, *12*, 5462.
- (15) (a) Umeda, N.; Tsurugi, H.; Satoh, T.; Miura, M. *Angew. Chem., Int. Ed.* **2008**, *47*, 4019. (b) Morimoto, K.; Hirano, K.; Satoh, T.; Miura, M. *Org. Lett.* **2010**, *12*, 2068. (c) Wang, F.; Song, G.; Li, X. *Org. Lett.* **2010**, *12*, 5430.
- (16) Schipper, D. J.; Hutchinson, M.; Fagnou, K. *J. Am. Chem. Soc.* **2010**, *132*, 6910.
- (17) For pioneering work employing catalytic copper and air as the terminal oxidant, see ref 9.
- (18) This aspect of the chemistry was identified in a *Synfacts* Highlight of our previously reported indole synthesis, ref 10b. *Synfacts* **2009**, 3, 254.

- (19) Li, L.; Brennessel, W. W.; Jones, W. D. *Organometallics* **2009**, *28*, 3492.

ability to elaborate the primary reaction products into pyrroles with a variety of substitution patterns.

Results and Discussion

Indole Formation: Reaction Development. In the coupling of acetanilide **4a** with 1-phenyl-1-propyne **5a**, our previous optimization identified the requirement for a silver additive to sequester chloride anions from precatalyst **1** in order to obtain catalytic activity.^{10b} The secondary investigation of reaction conditions presented here focused on the use of molecular oxygen as the terminal oxidant in conjunction with a catalytic amount of a transition metal oxidant. In order to do so, we first explored the effect of reaction temperature and have found that it can be reduced to 60 °C with a concomitant increase in reaction time, resulting in an improved yield of **6a** (Table 1, entries 1 and 2). Employing 10 mol % copper(II) acetate with a balloon of oxygen, we were pleased to find that we could still obtain moderate yields of **6a** (Table 1, entry 3). Additionally, the reaction yield could be restored to synthetically useful levels by further increasing the reaction time to 22 h and slightly increasing the loading of copper(II) acetate to 20 mol % (Table 1, entries 4 and 5). These studies also identified **2** as a competent catalyst precursor for this reaction,²⁰ providing **6a** in excellent yield while simplifying the reaction setup (Table 1, entry 6). The bench-stable powder **2** is easily prepared, may be weighed out to air, is insensitive to oxygen and moisture, and provides the advantage of avoiding the use of hygroscopic AgSbF₆. When the reaction was carried out at room temperature (21 °C) under the otherwise optimized conditions of entry 6 in Table 1, the yield reached 9% and 12% after 30 and 96 h, respectively (Table 1, entries 7 and 8). These low yields were likely due to the insolubility of many of the reaction components in *t*-AmOH at room temperature; however, over an extended period of time (96 h), a GCMS yield of 95% was obtained in acetone as the solvent at 21 °C (Table 1, entry 9). This result demonstrates the robust nature of the catalyst such that even after 4 days, catalytic turnover was observed. In the context of developing an overnight reaction, the conditions described in entry 6 were taken as optimal and used in further investigations of the general utility of the reaction.²¹ We have also explored the effect of the aniline-nitrogen protecting group and found that in the absence of a protecting group no reaction was observed. Additionally, while more sterically encumbered *N*-pivaloylaniline provides a diminished yield of the desired indole, the use of substrates with attenuated Lewis basicity at the amide oxygen, such as *N*-trifluoroacetylaniline and *N*-Boc-aniline, were ineffective in providing any appreciable amount of **6a**.

Indole Formation: Reaction Scope and Limitations. Having arrived at mild second-generation conditions, we now report the full compatibility of the reaction with respect to both the acetanilide and alkyne coupling partners under both first- and second-generation conditions. When various acetanilides were examined, yields were generally comparable or better under the second-generation conditions (for example **6a** is prepared in 79% and 90% yield under first- and second-generation conditions,

respectively, compare entries 1 and 6, Table 1). Additionally, a multitude of 5-, 6-, and 7-substituted indoles were readily prepared using this reaction. Para-substituted acetanilides bearing electron-donating, electron-withdrawing, and halide substituents afforded the corresponding 5-substituted indoles **6b–f** in good yields (Chart 1, entries 1–5). Meta-substitution was tolerated in the case of both symmetrical and unsymmetrical acetanilides. Electron-rich and electron-poor 3,5-substituted acetanilides gave 4,6-disubstituted indoles **6g** and **6i** in good yields (Chart 1, entries 6 and 8). However, it was evident that steric effects play a significant role in reaction efficiency, as 3,5-dimethylacetanilide provided indole **6h** in very low isolated yield (7%), even under extended reaction times (Chart 1, entry 7). When 3-substituted acetanilides were employed, the inherent regioselectivity of the reaction was for the more sterically accessible C–H bond. Steric effects dominate this process over electronic effects, as **6k** was produced as a *single regioisomer* in good isolated yield (Chart 1, entry 10). Other electronically diverse meta-substituted acetanilides also react at the more sterically accessible C–H bond to furnish 6-substituted indoles. An electron-donating methoxy group was compatible, providing good isolated yield of the 6-substituted indole **6j** as the major regioisomer (Chart 1, entry 9). The slightly diminished yield under the second-generation conditions likely reflected the reduced regioselectivity under these conditions (*vide infra*). An acetanilide bearing an electron-withdrawing substituent, such as a methyl ester, reacted with regioselectivity consistent with other meta-substituted acetanilides, but with much lessened reactivity, producing indole **6l** in 22% isolated yield (Chart 1, entry 11). Additionally, a benzo-fused acetanilide provided the corresponding indole in good yield (Chart 1, entry 12). Ortho-substitution was also tolerated yielding 7-methyl-substituted or benzo[*g*]indoles, **6n**, and **6o**, respectively (Chart 1, entries 13 and 14).

A range of new and functionally diverse alkynes were compatible under our second-generation conditions (Chart 2). As previously observed, both aryl/aryl and alkyl/alkyl symmetrically substituted internal alkynes produced 2,3-disubstituted indoles **7b** and **7c** in moderate to excellent yields, with the second-generation conditions providing enhanced yield in the case of the former (Chart 2, entries 1 and 2). However, when an unsymmetrical alkyl/alkyl substituted internal alkyne was employed in the reaction, a mixture of C2/C3 indole regioisomers was obtained (Chart 2, entry 3). In this case, a low yield was observed and while the regioselectivity of alkyne insertion was low (1.2:1), it was consistent with other rhodium(III)-catalyzed annulations.^{10b,13b,14c} Given the significant challenge in the preparation of this class of compound by transition metal-catalyzed annulations of internal alkynes, continued research will be necessary to find a synthetically useful solution to the formation of unsymmetrical 2,3-dialkylindoles. Conversely, alkyl/aryl internal alkynes reacted with near exclusive regioselectivity (>40:1), placing the aryl substituent proximal to the indole nitrogen. A number of different functional groups, including an electron-donating group, **7f**, and a halide, **7g**, were compatible on the aryl moiety of this class of alkyne (Chart 2, entries 5 and 6). Unsaturated heterocycles, such as thiophene, **7h**, and indole, **7i**, may also serve as the aryl moiety, providing a heterobiaryl linkage at the C2 position of indole in good yields (Chart 2, entries 7 and 8). The mild second-generation conditions allowed for additional functional groups on the alkyl moiety of alkyl/aryl internal alkynes. A cyclic alkyl group, such as cyclopropyl, led to 3-cyclopropylindole **7j** in moderate yield

(20) Subsequent to its use in our indole forming reaction, catalyst **2** has been utilized in the synthesis of isoquinolines (ref 13b) and in the hydroarylation of unactivated alkynes (ref 16) by our group. This catalyst (**2**) will soon be commercially available from Strem Chemicals, Inc.

(21) It should be noted that the reaction set-up is operationally very simple and that there is no need for special precautions to exclude atmospheric air or moisture.

Chart 1. Acetanilide Compatibility under Both First- and Second-Generation Conditions

Entry	Acetanilide	Alkyne	Product ^b	Entry	Acetanilide	Alkyne	Product ^b
1		5a	 82%, 76%	8		5a	 74%
2		5a	 47%, 74%	9		5a	 73%(9:1) ^c , 67%(6:1) ^d
3		5a	 62%, 78%	10		5a	 78%
4		5a	 69%	11		5a	 22%
5		5a	 89%	12		5a	 62%
6		5a	 70%, 69%	13		5a	 66%, 72%
7		5a	 7%	14		5a	 72%

^a Conditions: First generation (red): Acetanilide (1 equiv 0.2 M), **5a** (1.1 equiv), **1** (2.5 mol %), AgSbF₆ (10 mol %), Cu(OAc)₂·H₂O (2.1 equiv), *t*-AmOH, 120 °C, 1–3 h. Second generation (blue): Acetanilide (1 equiv 0.2 M), **5a** (1.1 equiv), **2** (5 mol %), Cu(OAc)₂·H₂O (20 mol %), O₂ balloon, *t*-AmOH, 60 °C, 20 h. ^b Isolated yields are reported above. ^c Regioselectivity based on isolated yield of regioisomers. ^d Regioselectivity based on crude ¹H NMR spectrum.

(Chart 2, entry 9). Ethyl propiolate esters, 3-alkynoates, and a diethylmalonate moiety at the propargylic position of the alkyne were all tolerated, providing functionalized indoles in moderate to good yields (Chart 2, entries 10–12). Unfortunately, under both first- and second-generation conditions, terminal alkynes were incompatible, largely producing alkyne homocoupling products. However, while the reaction yield was low, TMS-substituted 1-octyne **5o** reacted with acetanilide **4a** under modified second-generation conditions to yield the indole product, **7o**, with the TMS group proximal to the indole nitrogen. This provides the opportunity for TMS-group cleavage from the indole product and the ability to access C2 unsubstituted indoles.

Unprotected propargyl alcohols were unreactive when subjected to either set of reaction conditions. Thus, an investigation of common protecting groups was conducted to allow for the use of this important class of compound (Table 2). These studies found that a competitive solvolysis of the indole product was

occurring, producing C3-benzyl ether **8**.²² In *t*-AmOH this process was largely dependent on the nature of the protecting group and a screen of common alcohol protecting groups proved most fruitful. Due to its good leaving group ability, the use of acetate as a protecting group resulted in the significant production of **8** (Table 2, entry 2). Although the use of benzyl and silyl groups equally reduced the production of the solvolysis product, *tert*-butyldimethylsilyl-protected alcohol provided the desired product in the highest yield (Table 2, entries 3–5). Furthermore, control experiments revealed that **8** was observed when indole products **7q–t** were heated alone in *tert*-amyl alcohol.²³ The use of a TBS-protecting group could also be extended to include protected homopropargyl alcohols as coupling partners in good yield (Chart 2, entry 13).

(22) Other solvents were tested in order to avoid solvolysis of the product with *t*-AmOH. However, slow reactions and lower yields of the desired product were observed.

(23) See Supporting Information for further details.

Chart 2. Alkyne Compatibility under Both First- and Second-Generation Conditions

Entry	Acetanilide	Alkyne	Product ^b	Entry	Acetanilide	Alkyne	Product ^b
1	4a	5b	7b 81%, 90%	8	4a	5i	7i 81%
2	4a	5c	7c 68%, 67%	9	4a	5j	7j 50%
3	4a	5d	7d 44% ^c (51%; 1.2:1) ^d	10	4a	5k	7k 57%
4	4a	5e	7e 83%	11	4a	5l	7l 85%
5	4a	5f	7f 70%	12	4a	5m	7m 83%
6	4a	5g	7g 73%	13	4a	5n	7n 82%
7	4a	5h	7h 71%	14	4a	5o	7o 20% ^e

^a Conditions: First generation (red): 4a (1 equiv. 0.2 M), alkyne (1.1 equiv.), 1 (2.5 mol %), AgSbF₆ (10 mol %), Cu(OAc)₂·H₂O (2.1 equiv.), *t*-AmOH, 120 °C, 1–3 h. Second generation (blue): 4a (1 equiv. 0.2 M), alkyne (1.1 equiv.), 2 (5 mol %), Cu(OAc)₂·H₂O (20 mol %), O₂ balloon, *t*-AmOH, 60 °C, 20 h. ^b Isolated yields are reported above. ^c Isolated yield of a mixture of regioisomers (major isomer shown). ^d Yield of mixture of regioisomers and ratio based on crude ¹H NMR spectrum vs trimethoxybenzene as internal standard. ^e *i*-PrOAc used as solvent.

^a Conditions: First generation (red): 4a (1 equiv. 0.2 M), alkyne (1.1 equiv.), 1 (2.5 mol %), AgSbF₆ (10 mol %), Cu(OAc)₂·H₂O (2.1 equiv.), *t*-AmOH, 120 °C, 1–3 h. Second generation (blue): 4a (1 equiv. 0.2 M), alkyne (1.1 equiv.), 2 (5 mol %), Cu(OAc)₂·H₂O (20 mol %), O₂ balloon, *t*-AmOH, 60 °C, 20 h. ^b Isolated yields are reported above. ^c Isolated yield of a mixture of regioisomers (major isomer shown). ^d Yield of mixture of regioisomers and ratio based on crude ¹H NMR spectrum vs trimethoxybenzene as internal standard. ^e *i*-PrOAc used as solvent.

Table 2. Screen of Potential Propargyl Alcohol Protecting Groups

entry	alkyne	R group	yield ^b of 7p–t	yield ^b of 8
1	5p	H	7p: —	—
2	5q	Ac	7q: 16%	59%
3	5r	Bn	7r: 35%	11%
4	5s	TBS	7s: 67%	11%
5	5t	TIPS	7t: 35%	17%

^a Conditions: 4a (1 equiv., 0.2 M), alkyne (1.1 equiv.), 2 (5 mol %), Cu(OAc)₂·H₂O (20 mol %), O₂ balloon, *t*-AmOH, 60 °C, 20 h. ^b Isolated yields.

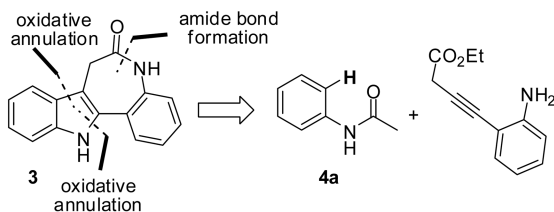
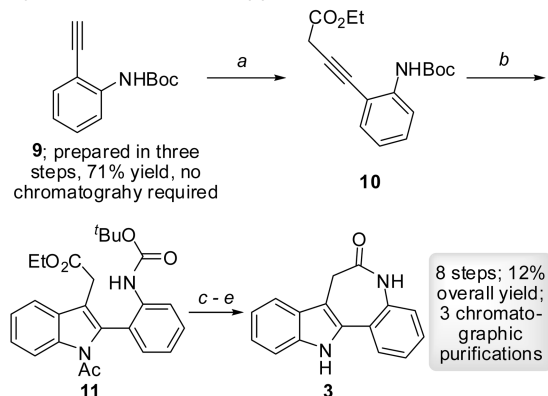
Synthetic Applications: Synthesis of Paullone. Having established a method to efficiently construct indoles with high functional group compatibility, we investigated the feasibility of applying our method to the synthesis of paullone 3. The paullone family of compounds was originally discovered by Sausville during studies on a semisynthetic flavinoid, flavopiridol, known to inhibit cyclin-dependent kinases (CDKs) 1, 2, and 4.²⁴ Over the past decade, numerous derivatives of paullone have been found to possess biological activity similar to that of CDK-1, -2, and -5 inhibitors,²⁵ to have in vitro antitumor

(24) Sausville, E. A.; Zaharevitz, D.; Gussio, R.; Meijer, L.; Louarn-Leost, M.; Kunick, C.; Schultz, R.; Lahusen, T.; Headlee, D.; Stinson, S.; Arbus, S. G.; Senderowicz, A. *Pharmacol. Ther.* **1999**, 82, 285.

(25) Zaharevitz, D.; Gussio, R.; Leost, M.; Senderowicz, A.; Lahusen, T.; Kunick, C.; Meijer, L.; Sausville, E. A. *Cancer Res.* **1999**, 59, 2566.

Scheme 2. Retrosynthesis and Forward Synthetic Route to Paullone **3**^a

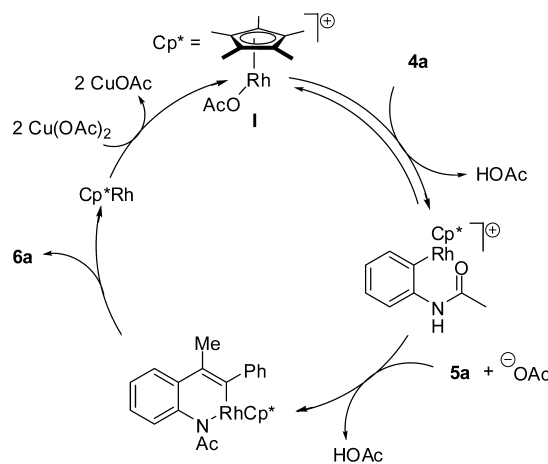
Retrosynthetic analysis:

Synthetic route to Paullone (**3**):

^a Conditions: (a) **9** (1 equiv), ethyl diazoacetate (1.05 equiv, 0.8 M), CuI (10 mol %), MeCN, r.t., 12 h; 70%. (b) **4a** (1 equiv, 0.2 M), **10** (1.1 equiv), **2** (5 mol %), Cu(OAc)₂·H₂O (20 mol %), O₂ (atm), *t*-AmOH, 60 °C, 20 h; 71%. (c) **11** (1 equiv), K₂CO₃ (10 equiv), MeOH:DCM (1:1), r.t., 12 h; 97%. (d) TFA (0.1 M), r.t., 30 min; 94%. (e) DBU (1.2 equiv), DMF (0.1 M), 150 °C, 19 h; 36% (33% over three steps).

activity,²⁶ in vitro antiproliferative activity,²⁷ and antileishmanial activity,²⁸ and to inhibit glycogen synthase kinase-3 (GSK-3), which may find use in the treatment of diabetes.²⁹ As such, there has been a significant effort directed toward efficient syntheses of this class of compounds.³⁰

The majority of previous routes toward paullone (or its derivatives) are initiated with a preformed indole which is therein functionalized during the synthesis.^{30a,b,d,e} Our group's interest in the synthesis of heterocycles via reactions that take place at C–H bonds and the lack of synthetic routes for the construction of the indole from simple starting materials prompted us to develop an efficient route to paullone **3**, employing the oxidative coupling of acetanilide **4a** and an appropriately functionalized alkyne (Scheme 2). There was sufficient literature precedent from previous paullone syn-

Scheme 3. Proposed Catalytic Cycle under Our First-Generation Conditions


theses^{30a,c,f} that the azepine ring may be closed by intramolecular amide bond formation from the corresponding aniline and benzylic ester (or equivalent carbonyl). Thus, our retrosynthesis was reduced to the formation of the appropriately substituted indole, which could arrive from the coupling of **4a** and an appropriately functionalized alkyne **10** (Scheme 2).

Alkyne **10** was prepared in four steps in 50% overall yield with chromatographic purification necessary only after the final step (Scheme 2).²³ The alkyne was then set for oxidative coupling with **4a** under the second-generation conditions, yielding indole **11** in 71% isolated yield. As previously observed in a screen of compatible nitrogen protecting groups, exclusive chemoselectivity was observed for reaction with rhodium at the acetanilide in the presence of the *N*-Boc-aniline, two functional groups with significant structural similarity. Following chromatographic purification, and with the indole core set, the final sequence of reactions was carried out in three steps. Treatment of **11** with K₂CO₃ in MeOH/DCM followed by acidic (TFA) cleavage of the Boc group affords the unprotected indole and aniline. Exposure of the crude product to basic (DBU) conditions effects an intramolecular amide bond formation, affording paullone **3** in 33% yield from **11** and 12% overall yield from commercially available compounds in eight steps using only three chromatographic purifications (Scheme 2).

Mechanistic Investigation. A general catalytic cycle, under our first-generation conditions, is shown in Scheme 3 based on our previous preliminary mechanistic investigation^{10b} and the proposals put forth by Larock^{5g} as well as Satoh and Miura for other annulative processes with internal alkynes.⁹ Jones has revealed that the active metalating agent in the stoichiometric cyclometalation of benzylimines with [Cp*RhCl₂]₂ **1** was the cationic complex **I** (Scheme 3).¹⁹ Given the similarity of our reaction and the large excess of acetate in our first-generation conditions, we propose a similar scenario for this reaction. Complex **I** is presumably generated from the combination of catalyst precursor **1**, AgSbF₆, and acetate (from Cu(OAc)₂) and, based on our previous work, reversibly metalates acetanilide to form a cyclometalated intermediate. Alkyne coordination to rhodium and 1,2-migration of the rhodium–carbon bond across the alkyne results in the formation of the requisite carbon–carbon bond and a six-membered metallacycle. The carbon–nitrogen bond of the indole product is formed after reductive elimination, at which time the metal catalyst is reduced to Rh(I). Reoxidation of the reduced catalyst with the copper(II) oxidant restores the catalytically active rhodium(III)-complex (Scheme 3).

- (26) Schultz, C.; Link, A.; Leost, M.; Zaharevitz, D.; Gussio, R.; Sausville, E. A.; Meijer, L.; Kunick, C. *J. Med. Chem.* **1999**, *42*, 2909.
 (27) Kunick, C.; Schultz, C.; Lemcke, T.; Zaharevitz, D.; Gussio, R.; Jalluri, R. K.; Sausville, E. A.; Leost, M.; Meijer, L. *Bioorg. Med. Chem. Lett.* **2000**, *10*, 567.
 (28) Reichwald, C.; Shimony, O.; Dunkel, U.; Sacerdoti-Sierra, N.; Jaffe, C. L.; Kunick, C. *J. Med. Chem.* **2008**, *51*, 659.
 (29) Stukenbrock, H.; Musmann, R.; Geese, M.; Ferandin, Y.; Lozach, O.; Lemcke, T.; Kegel, S.; Lomow, A.; Burk, U.; Dohrmann, C.; Meijer, L.; Austen, M.; Kunick, C. *J. Med. Chem.* **2008**, *51*, 2196.
 (30) For previous syntheses of paullone and its derivatives, see: (a) Baudoin, O.; Cesario, M.; Guénard, D.; Guéritte, F. *J. Org. Chem.* **2002**, *67*, 1199. (b) Bremner, J. B.; Sengpracha, W. *Tetrahedron* **2005**, *61*, 5489. (c) Henry, N.; Blu, J.; Bénateau, V.; Mérour, J.-Y. *Synthesis* **2006**, 3895. (d) Avila-Zárraga, J. G.; Lujan-Montelongo, A.; Covarrubias-Zúñiga, A.; Romero-Ortega, M. *Tetrahedron Lett.* **2006**, *47*, 7987. (e) Joucla, L.; Popowycz, F.; Lozach, O.; Meijer, L.; Joseph, B. *Helv. Chem. Acta* **2007**, *90*, 753. (f) Tobisu, M.; Fujihara, H.; Koh, K.; Chatani, N. *J. Org. Chem.* **2010**, *75*, 4841.

Table 3. Temperature-Dependence of the Reversibility of the Cyclorhodation

entry	conditions	temp, °C	%H incorporation ^b	
			4a-d _n	6a-d _n
1	A	120	75	27
2	B	90	20	4
3	B	60	0	0
4 ^c	B	60	>90	—

^a Conditions: A: **4a-d₅** (1 equiv, 0.2 M), **5a** (1.1 equiv), **1** (2.5 mol %), AgSbF₆ (10 mol %), Cu(OAc)₂·H₂O (2.1 equiv), *t*-AmOH, 120 °C, 4 min. B: **4a-d₅** (1 equiv, 0.2 M), **5a** (1.1 equiv), **2** (5 mol %), Cu(OAc)₂·H₂O (20 mol %), O₂ balloon, *t*-AmOH, 60 or 90 °C, 5 h.

^b Reactions were stopped at ~50% conversion, and % H incorporation was determined by ¹H NMR spectroscopy on pure isolated material.

^c No alkyne **5a** added to reaction mixture.

We have identified the current limitations of the more mild second-generation conditions to include the poor reactivity of alkyl/alkyl-substituted internal alkynes, very low regioselectivity for unsymmetrical alkyl/alkyl-substituted internal alkynes, and reduced regioselectivity of meta-substituted acetanilides relative to the first-generation conditions. Subsequent to the development of our second-generation conditions, the mechanism of the reaction was explored in order to verify our initial proposal and address these limitations. We primarily employed kinetic analysis of the reagents and isotope labeling experiments to gain insight into these aspects of the chemistry and, where applicable, to aid in the development of improved reaction conditions for these processes.

Reversibility of Acetanilide Cyclorhodation and the Presence of a Primary DKIE. Our previous study^{10b} found that, under the first-generation conditions, the acetanilide cyclorhodation was a reversible process, resulting in 75% loss of deuterium exclusively ortho to the amide using **4a-d₅** (Table 3, entry 1). These results suggested that the metalation is directed by the Lewis basic amide group and are not in line with traditional Friedel–Crafts chemistry. Further experiments were carried out to determine if this was also true of the more mild second-generation conditions. Indeed, it was found that the cyclorhodation was intrinsically reversible in the absence of alkyne under the second-generation conditions (Table 3, entry 4). However, with all reaction components present, the metalation of acetanilide was found to be irreversible, with no loss in deuterium from **4a-d₅** (Table 3, entry 3). Interestingly, a trend of decreasing reversibility of metalation (H incorporation) with decreasing temperature was observed (Table 3, entries 1–3).

The irreversibility of the C–H bond functionalization event under the more mild conditions prompted us to investigate the presence of a deuterium kinetic isotope effect (DKIE). The average initial rate of the reaction was $3.1 (\pm 0.5) \times 10^{-4}$ M/s using acetanilide **4a** and $0.74 (\pm 0.09) \times 10^{-4}$ M/s using acetanilide **4a-d₅**. A comparison of these initial rates revealed a primary DKIE of 4.2 ± 0.9 , suggesting that the rate-determining step involved rhodium-catalyzed C–H bond cleavage (eq 5). Additionally, a DKIE of this magnitude is consistent with a concerted metalation–deprotonation (CMD) mechanism being operative in this process. Furthermore, this data, in

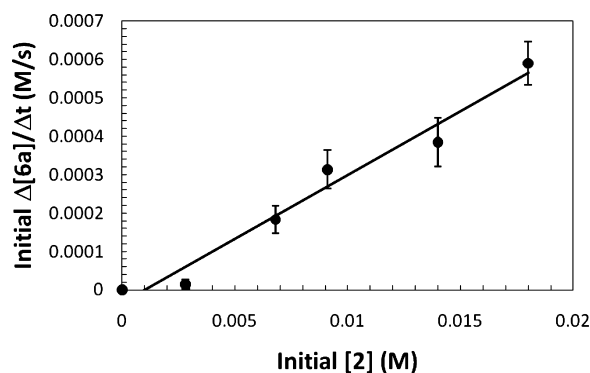
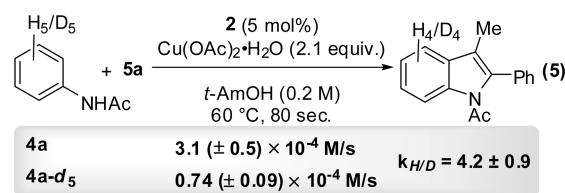


Figure 2. Kinetic plot for rate dependence on the concentration of **2**. Conditions: **4a** (1 equiv, 0.15 M), **5a** (1.1 equiv), **2** (0–0.018 M), Cu(OAc)₂·H₂O (2.1 equiv), trimethoxybenzene (1 equiv) as internal standard, *t*-AmOH, 60 °C, 80 s.

conjunction with other experimental data obtained,³¹ is in accord with previous experimental^{19,32} and computational findings³³ for a CMD mechanism in other cyclometalation reactions.³⁴



Determination of the Order of Reagents. Our kinetic analysis commenced with the determination of the rate order of each of the primary reaction components (catalyst, acetanilide, and alkyne) under the second-generation conditions.³⁵ The reaction conditions used in the kinetic analysis were a slight modification of the second-generation conditions such that 2 equiv of the Cu(OAc)₂·H₂O oxidant was employed in place of 20 mol % Cu(OAc)₂·H₂O and an oxygen atmosphere.³⁶ First-order dependence of the reaction rate on rhodium concentration was obtained from the linear plot of initial rate ($\Delta[6a]/\Delta t$) vs initial rhodium concentration ([**2**]) (Figure 2). Saturation kinetics were observed with respect to acetanilide concentration when similar experiments were carried out by measuring the initial rate over a range of **4a** concentrations (Figure 3). These combined data advocate that the acetanilide reversibly binds to rhodium, most likely via its Lewis basic amide oxygen, before the rate-determining step, and are consistent with the catalyst and acetanilide being saturated as a coordination complex prior to irreversible and rate-determining C–H bond cleavage.

(31) A Hammett correlation and an Arrhenius plot are also provided in the Supporting Information.

(32) Ryabov, A. D.; Sakodinskaya, I. K.; Yatsimirsky, A. K. *J. Chem. Soc., Dalton Trans.* **1985**, 2629.

(33) (a) Davies, D. L.; Donald, S. M. A.; Macgregor, S. A. *J. Am. Chem. Soc.* **2005**, *127*, 13754. (b) Davies, D. L.; Donald, S. M. A.; Al-Duaij, O.; Macgregor, S. A.; Pölleth, M. *J. Am. Chem. Soc.* **2006**, *128*, 4210.

(34) For a historical perspective on the evolution of the CMD mechanism in the chemical literature, including examples involving cyclometalation reactions, see: Lapointe, D.; Fagnou, K. *Chem. Lett.* **2010**, *39*, 1118.

(35) See the Supporting Information for exact details of data collection for the kinetic experiments.

(36) This modification to the second-generation reaction conditions was done for practical purposes of data collection and determined to be insignificant to initial rate determinations because under a relevant concentration range (0.2–2.1 equiv) of Cu(OAc)₂·H₂O, the reaction rate exhibited zero-order dependence on [Cu(OAc)₂]; see Supporting Information for more details.

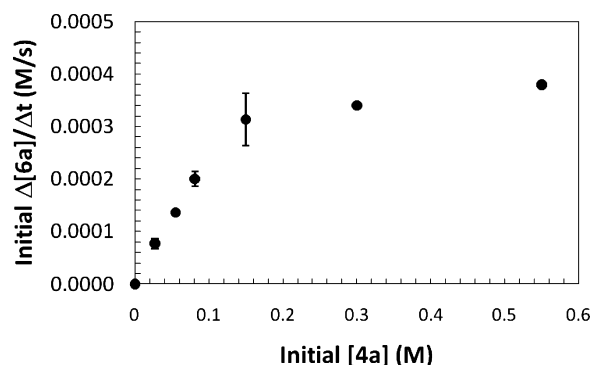


Figure 3. Kinetic plot for rate dependence on the concentration of **4a**. Conditions: **4a** (0–0.55 M), **5a** (1 equiv, 0.17 M), **2** (5 mol %), Cu(OAc)₂·H₂O (2.1 equiv), trimethoxybenzene (1 equiv) as internal standard, *t*-AmOH, 60 °C, 80 s.

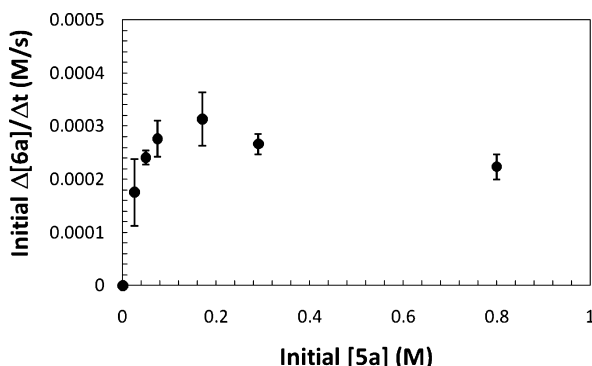


Figure 4. Kinetic plots for rate dependence on the concentration of **5a**. Conditions: **4a** (1 equiv, 0.15 M), **5a** (0–0.8 M), **2** (5 mol %), Cu(OAc)₂·H₂O (2.1 equiv), trimethoxybenzene (1 equiv) as internal standard, *t*-AmOH, 60 °C, 80 s.

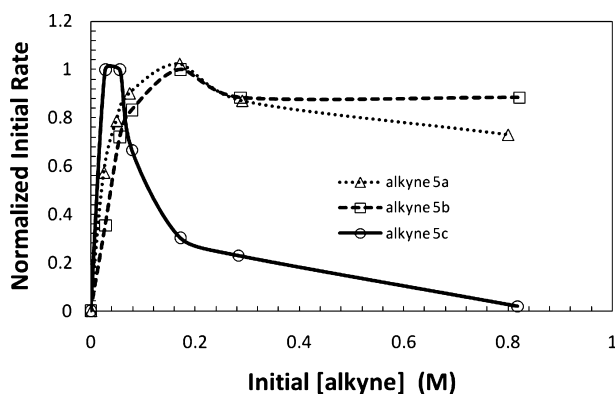


Figure 5. Normalized kinetic plots for the rate dependence on the concentration of alkynes **5a–c**.

A sharp increase in reaction rate followed by a region of rate inhibition at high alkyne concentrations was observed when a similar analysis was carried out over a range of alkyne **5a** concentrations (0–0.80 M, Figure 4). Given this unanticipated result, alkynes **5b** (diphenylacetylene) and **5c** (4-octyne) were subjected to analogous inspection in order to determine if this effect was a general phenomenon common to other alkynes over the same concentration range. Figure 5 shows a plot of normalized initial rate vs alkyne concentration for alkynes **5a**, **5b**, and **5c**.³⁷ While the general behavior of a sharp rate increase followed by a region of rate inhibition is consistent across the three alkynes, the magnitude of rate inhibition and shape of the curves varies significantly. Similar kinetic behavior was ob-

Table 4. DKIEs for a Range of Alkynes and Alkyne Concentrations

entry	alkyne	[alkyne]	DKIE	product
1	5a	0.17 M	4.2 ± 0.9	6a
2	5b	0.17 M	3.6	7b
3	5c	0.17 M	3.5	7c
4	5a	0.05 M	3.5 ± 0.2	6a
5	5a	0.80 M	3.0 ± 0.5	6a

^a Conditions: **4a** or **4a-d₅** (1 equiv, 0.15 M), alkyne (see above for concentration), **2** (5 mol %), Cu(OAc)₂·H₂O (2.1 equiv), *t*-AmOH, TMB = trimethoxybenzene (1 equiv) as internal standard, 60 °C, 80 s.

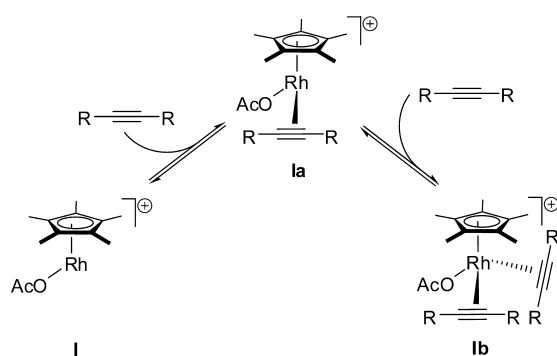
served for alkynes **5a** and **5b**, with alkyne **5a** inhibiting the reaction rate to a slightly greater extent at high alkyne concentration (0.8 M). However, alkyne **5c**, while also having a sharp increase in rate at very low alkyne concentrations (<0.04 M), displayed a more drastic rate inhibition at higher alkyne concentrations (>0.08 M, Figure 5). The presence of a primary DKIE (4.2 ± 0.9 at 0.15 M acetanilide, eq 5) was used to probe the unusual observed rate dependence on alkyne concentration and the fidelity of the rate-determining step over alkynes **5a**, **5b**, and **5c**, under relevant concentrations (Table 4). These experiments demonstrate that the rate-determining step is invariable for the reactions with these alkynes due to a consistent and large primary DKIE of ~3.6 (Table 4, entries 1–3). Additionally, over the alkyne concentrations used in our kinetic study, there is little variation in the DKIE, which remains significantly large (Table 4, entries 1, 4, and 5). This suggests that the nature and mechanism of the rate-determining step of the reaction is unchanged over these alkyne concentrations and remains the C–H bond cleavage step.

Within the catalytic cycle, 1,2-migratory insertion of the rhodium–carbon arene bond across the alkyne takes place after the rate-determining C–H bond cleavage step, and therefore, in this case, zero-order dependence of the reaction rate on alkyne concentration would be expected (Scheme 3). However, the observed kinetic data with respect to alkyne concentration was certainly not zero order and indicated a noninteger dependence of the reaction rate on alkyne concentration suggesting an additional role for this component prior to the rate-determining step. Kinetic profiles of this type have been observed in other transition metal and organocatalyzed processes³⁸ and have been attributed to an inhibitory binding event of the reagent in question (alkyne in this case) to the active catalyst prior to the rate-determining step. Cognizant of these precedents, we propose a similar scenario for this reaction in which the alkyne reversibly coordinates the active catalyst **I**, effectively occupying the free coordination site necessary for C–H bond cleavage (Scheme 4). The shape of the curves in Figure 5 also indicate that the stoichiometry of the rhodium–alkyne complexes formed are not limited to a 1:1 complex and may differ for the three alkynes examined.

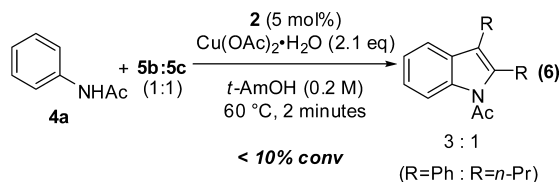
Interestingly a one-pot competition experiment between the two alkynes at either end of the spectrum of rate inhibition (**5b**

(37) The lines drawn in Figure 5 are done in order to guide the reader's eye and do not represent a mathematical correlation.

(38) (a) Steinhoff, B. A.; Guzei, I. A.; Stahl, S. S. *J. Am. Chem. Soc.* **2004**, *126*, 11268. (b) Schultz, M. J.; Adler, R. S.; Zierkiewicz, W.; Privalov, T.; Sigman, M. S. *J. Am. Chem. Soc.* **2005**, *127*, 8499. (c) Zuend, S. J.; Jacobsen, E. N. *J. Am. Chem. Soc.* **2007**, *129*, 15872.

Scheme 4. Proposed Source of Rate Inhibition by Alkynes

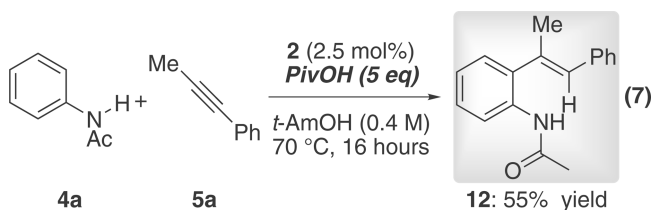
and **5c**) revealed a preference for migratory insertion across the diaryl alkyne **5b** over the dialkyl alkyne **5c** (eq 6). This competition experiment removes any ambiguity due to rate inhibition and directly demonstrates the preference for migratory insertion across the diaryl alkyne despite the stronger interaction between rhodium and the dialkyl alkyne implicit from Figure 5. This is consistent, though to a lesser degree, with a previous observation by Rovis for a related Rh(III)-catalyzed annulation of internal alkynes in which exclusive reaction with diphenylacetylene was observed in the presence of an equimolar quantity of 5-decyne.^{14c} This observation corroborates the empirically observed lower yields for dialkyl alkynes in these transformations due to a competitive off-cycle inhibitory pathway that is much more pronounced for this class of alkyne in comparison to diaryl alkynes.



Isolation and Characterization of a Reaction Side Product.

A significant amount of a side product was obtained when chlorinated solvents³⁹ were used during the optimization of our second-generation conditions. Isolation and structural characterization of the compound revealed it to be the hydroarylation product **12**. Intrigued by the fact that this trisubstituted alkene is produced as a single regio- and stereoisomer, we found that by removal of the oxidant and addition of a carboxylic acid⁴⁰ (5 equiv), modest yield of the hydroarylation product could be obtained (eq 7). This information assisted in the development of general conditions for the hydroarylation of unactivated alkynes with arenes and heteroarenes catalyzed by **2**.¹⁶ While the observation of **12** is further evidence that C–C bond formation precedes C–N bond formation, consistent with our proposed catalytic cycle, when **12** was subjected to our second-generation reaction conditions, none of the desired product **6a** was obtained. This result indicated that **12** is a nonproductive side product and not an intermediate en route to the desired indole, also consistent with our mechanistic proposal. Addition-

ally, under the optimized reaction conditions, the formation of **12** was typically less than 2%.



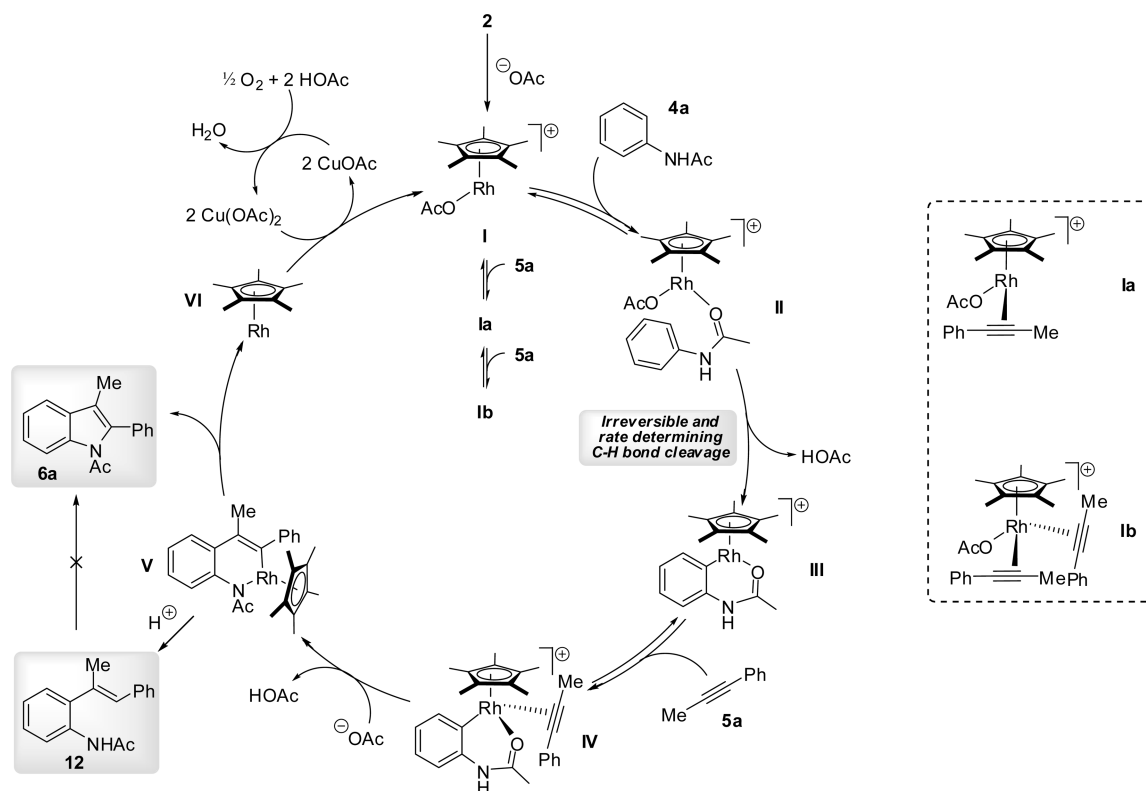
Revised Catalytic Cycle. The kinetic data obtained for this system is most consistent with the catalytic cycle depicted in Scheme 5. As previously postulated, complex **2** reacted with 1 equiv of acetate to form the active metalating agent **I**. However, **I** may react with alkyne **5a** in an inhibitory manner to form nonproductive coordination complexes **Ia** and **Ib**. The active catalyst **I** may also be coordinated by **4a** via the Lewis basic amide oxygen to form the coordination complex **II** which undergoes irreversible and rate-determining C–H bond cleavage producing **III**. Alkyne **5a** may then coordinate **III**, followed by carbo-rhodation to yield **V**. In the presence of adventitious acid, **V** may react to form the hydroarylation product **12**; however, this is a minor reaction pathway under our optimized conditions. C–N bond reductive elimination extrudes the desired indole product **6a** along with Cp*Rh(I). The reduced catalyst is then oxidized back to the active species via catalytic copper(II) acetate which is then reoxidized by the combination of molecular oxygen and acetic acid (generated in the reaction). Having established a viable catalytic cycle consistent with our kinetic data, we set out to investigate specific aspects of the reaction that we deemed were limitations of the chemistry, namely the regioselectivity of metalation of meta-substituted acetanilides and the regioselectivity of alkyne insertion into the rhodium–carbon bond of complex **III**.

Studies on the Regioselectivity of C–H Bond Functionalization Leading to Improved Conditions for Meta-Substituted Acetanilides. The first rhodium–carbon bond formation, resulting in **III**, was subject to issues of regioselectivity when meta-substituted acetanilides were used. This step consistently takes place at the more sterically accessible C–H bond of meta-substituted acetanilides regardless of the electronic character of the aromatic ring (Chart 1, entries 9–12). During our studies on the compatibility of the reaction conditions with various acetanilides, 3,5-dimethylacetanilide was found to be a poor substrate, resulting in only 7% isolated yield of the corresponding indole. Additionally, 3-methylacetanilide, **4k**, provided 6-methylindole, **6k**, in good yield as a single regioisomer, therefore implying that the acetanilide metalation step was extremely sensitive to steric effects. In a comparison of the first- and second-generation conditions with respect to regioselectivity at the acetanilide, indole **6j** was formed as a 9:1 mixture of regioisomers under the first-generation conditions, whereas the regioselectivity was reduced to 6:1 under the second-generation conditions. This result was consistent with the observed lack of reversibility of acetanilide metalation under the more mild temperatures of the second-generation conditions (see Table 3). In an effort to improve the site selectivity of acetanilide metalation under these mild conditions, we formally investigated the influence of temperature (Table 5) and alkyne concentration (Table 6) on regioselectivity. In line with our previous observations we found a small but consistent increase

(39) The greater formation of the side product in chlorinated solvents is attributed to the presence of small amounts of HCl due to decomposition of the solvent.

(40) The pK_a of the carboxylic acid was found to be critical to formation of **12**. Acids with $pK_a < 1$ resulted in very low conversion and a significant amount of **4a**. Acids with $pK_a > 1$ provided **12** in similar yield with pivalic acid giving optimal results; see the Supporting Information for further details.

Scheme 5. Revised Catalytic Cycle

Table 5. Influence of Temperature on Regioselectivity of Indole Formation with **4j**

entry	temp (°C)	¹ H NMR yield (%) ^b	6j (6-OMe:4-OMe) ^b
1	40	91	5.0:1
2	50	97	5.5:1
3	60	99	6.1:1
4	70	94	6.5:1
5	80	89	7.2:1

^a Conditions: **4j** (0.1 mmol, 0.2 M, 1 equiv), **5a** (0.11 mmol, 1.1 equiv), **2** (5 mol %), Cu(OAc)₂·H₂O (2.1 equiv), *t*-AmOH, temperature (see above). ^b Yield and ratio of mixture of 6-OMe and 4-OMe regioisomers determined by ¹H NMR spectroscopy versus 1,3,5-trimethoxybenzene as an internal standard.

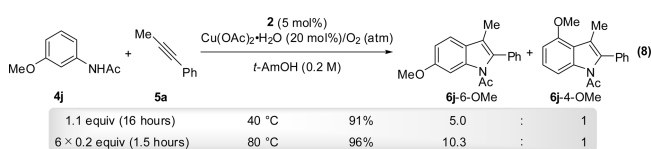
in regioselectivity over a range of increasing temperatures.⁴¹ Consequently, the regioselectivity was increased from 5:1 at 40 °C to ~7:1 at 80 °C (Table 5, compare entries 1 and 5). A much larger correlation between regioselectivity and initial alkyne concentration was observed when the reaction was carried out at 80 °C (Table 6). At low alkyne concentration, the regioselectivity is further increased to ~9:1, while, at high initial alkyne concentration (2M, 10 equiv of alkyne relative to acetanilide), the regioselectivity was dramatically reduced to 2.4:1. With this knowledge in hand, when the reaction was carried out at 80 °C with a portion-wise (0.2 equiv/~15 min) addition of the alkyne, an ~10:1 ratio and an excellent combined yield of 96% (by ¹H NMR) for the mixture of regioisomers was obtained (eq 8).⁴²

(41) This is opposite to what was previously observed by Jones for the stoichiometric cyclorhodation of benzylimines; see ref 19.

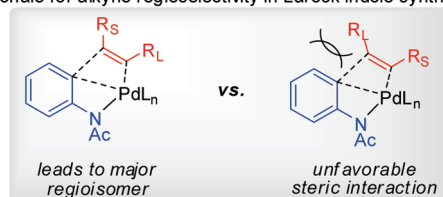
Table 6. Influence of Alkyne Concentration on Regioselectivity of Indole Formation with **4j**

entry	initial [5a] (M)	¹ H NMR yield (%) ^{b,c}	6j (6-OMe:4-OMe) ^b
1	0.04	17(85)	8.7:1
2	0.10	46(93)	7.4:1
3	0.23	89	7.2:1
4	1.00	84	3.0:1
5	2.00	84	2.4:1

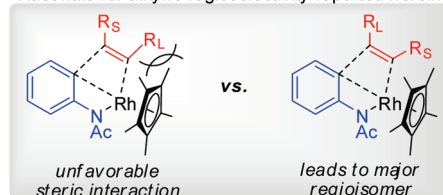
^a Conditions: **4j** (0.1 mmol, 0.2 M, 1 equiv), **5a** (see above for initial concentration), **2** (5 mol %), Cu(OAc)₂·H₂O (2.1 equiv), *t*-AmOH, 80 °C. ^b Yield and ratio of mixture of 6-OMe and 4-OMe regioisomers determined by ¹H NMR spectroscopy versus 1,3,5-trimethoxybenzene as an internal standard. ^c Yield in parentheses determined by ¹H NMR spectroscopy and based on the alkyne as the limiting reagent.



Studies on the Regioselectivity of the 1,2-Alkyne Migration Event. In contrast to the regioselectivity at the acetanilide, the effect of sterics appeared to have only a modest influence on the regioselectivity of the alkyne insertion (Chart 2, entry 3). Interestingly, the regioselectivity of this process was opposite to that previously reported by Larock.^{5g} In his account, Larock proposed that an unfavorable steric interaction between the larger alkyne substituent (R_L) and the aryl

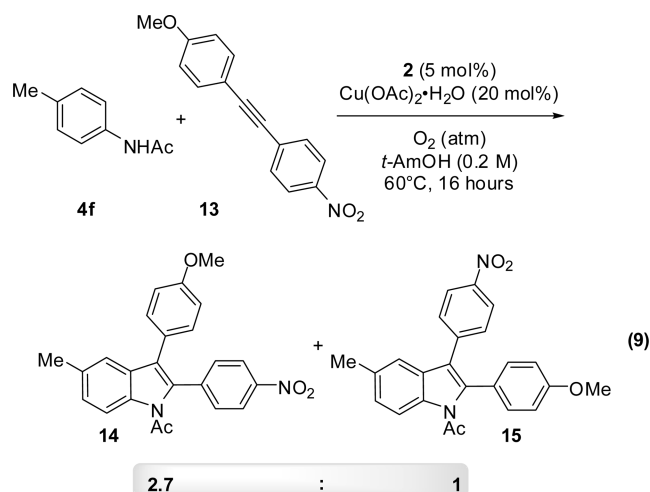
Scheme 6. Rationale for Regioselectivity of Alkyne Insertion Based on Steric EffectsRationale for alkyne regioselectivity in Larock indole synthesis⁵⁹

Rationale for alkyne regioselectivity reported herein

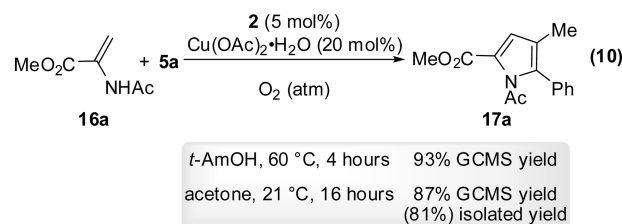


ring forced this substituent proximal to the indole nitrogen (Scheme 6). Whereas, in the reaction described in this report, we propose that the bulky pentamethylcyclopentadienyl (Cp*) ligand on rhodium forces the larger group to be distal to the indole nitrogen (Scheme 6). This result is consistent with the observed regioselectivity when unsymmetrical alkynes have been employed in other rhodium-catalyzed annulations with Cp*Rh(III)-catalysts.^{13b,14a,c}

The electronic effects of the alkyne substituents appear to have more influence over the regioselectivity of alkyne insertion than do the steric effects. This is particularly true when these two substituents have disparate electronic properties. Alkyne **13**, having two electronically distinct aryl groups, was prepared and subjected to the second-generation conditions in order to demonstrate the electronic bias for alkyne insertion (eq 9). The resulting mixture of indole regioisomers could not be separated by conventional chromatography; however, benzene-*d*₆ provided sufficient resolution in the ¹H NMR spectrum to allow for characterization of the mixture by 1D and 2D NMR methods.²³ The mixture of isomers was formed in a 2.7:1 ratio in favor of the electron-deficient aryl group proximal to the indole nitrogen.⁴³ In this specific case of alkyne **13**, adorned with two electronically dissimilar aryl substituents, the more electron-deficient substituent is delivered proximal to the indole nitrogen. However, this trend does not extend to the coupling of ethyl 3-phenylpropionate **5k** in which the more electron-withdrawing alkyne substituent (CO₂Et) is delivered distal to the indole nitrogen. Other interactions of the alkyne substituents with the catalyst may be operative in the case of **5k** (and related alkynes), overriding any inherent electronic bias of the alkyne insertion event.



Pyrrole Formation: Reaction Development. Despite the wide applicability of pyrroles in pharmaceuticals^{4,44} and biologically active natural products^{1c} and materials,² methods for their syntheses have not enjoyed the same level of ingenuity as those for their heterocyclic counterpart, the indole. Our development of mild conditions for the efficient synthesis of indoles and the broad substrate scope displayed by this reaction prompted us to explore the extension of this method to vinylic C–H bond functionalization in the context of a pyrrole synthesis.¹² A screen of a number of different enamides identified **16a** as a competent substrate for reaction development. When coupled with 1-phenyl-1-propyne **5a** under the reaction conditions described in entry 6 of Table 1, the desired pyrrole **17a** was obtained in 93% GCMS yield (eq 10). Encouraged by this result, the pyrrole formation was tested under the room temperature reaction conditions (21 °C in acetone as solvent; Table 1, entry 9), and, in this case, an 87% GCMS yield and 81% isolated yield was obtained after 16 h (eq 10). Furthermore, this reaction may be performed on gram-scale (1 g of **16a**), under reduced catalyst loading (3 mol % of **2**) with no loss in yield (80% isolated yield of **17a**).²³ Therefore, these two sets of conditions were used to test the generality of the reaction, primarily employing the room temperature conditions.



Pyrrole Formation: Reaction Scope and Limitations. While other processes of this nature have displayed a relatively limited substrate scope with respect to the alkyne,¹² the very mild reaction conditions developed here allow a wide variety of unactivated internal alkynes to be employed. Symmetrical diaryl and dialkyl internal alkynes reacted smoothly to afford pyrroles in moderate to excellent yields (Chart 3, entries 2 and 3). While a moderate 56% yield of 2,3-dialkyl-substituted pyrrole **17c** was obtained at room temperature, the yield was increased to a more synthetically useful 83% by employing conditions at a slightly higher temperature (60 °C in *t*-AmOH). In addition to 1-phenyl-1-propyne **5a** other alkyl/aryl unsymmetrical internal alkynes reacted well to give

(42) A method involving syringe pump addition of the alkyne was explored but was complicated by the small scale of the reaction. Therefore, syringe pump addition was abandoned for the sequential addition protocol.

(43) In the pyrrole forming reaction, a mixture of regioisomers in a 3.5:1 ratio is observed with the same selectivity as that observed in the indole-forming reaction.

(44) Fensome, A.; et al. *J. Med. Chem.* **2005**, *48*, 5092.

Chart 3. Enamide and Alkyne Compatibility in the Formation of Pyrroles

$\text{16a-e} + \text{Alkyne} \xrightarrow[\text{Acetone (0.2 M), 21 } ^\circ\text{C, 18 hours}^b]{\text{2 (5 mol\%), Cu(OAc)}_2\cdot\text{H}_2\text{O (20 mol\%), O}_2 \text{ (atm), } t\text{-AmOH (0.2 M) 60 } ^\circ\text{C, 4 hours}^a}$
 17a-p

Entry	Enamide	Alkyne	Product ^c	Entry	Enamide	Alkyne	Product ^c
1	16a	5a	17a 81%	9	16a	5s	17i 81%
2	16a	5b	17b 88%	10	16a	5w	17j 77%
3	16a	5c	17c 56%, 83%	11	16a	5o	17k 55% (over 2 steps) ^d
4	16a	5i	17d 70%	12	16a	5x	17l 76%
5	16a	5u	17e 62%	13	16b	5a	17m 71% ^e
6	16a	5v	17f 51%	14	16c	5a	17n 44% ^e
7	16a	5k	17g 82%	15	16d	5a	17o 26% ^e
8	16a	5l	17h 79%	16	16e	5a	17p 32% ^e

^a Conditions (at 60 °C; red): Enamide (1 equiv 0.2 M), alkyne (1.1 equiv), **2** (5 mol %), Cu(OAc)₂·H₂O (20 mol %), O₂ balloon, *t*-AmOH, at 60 °C, 4 h.

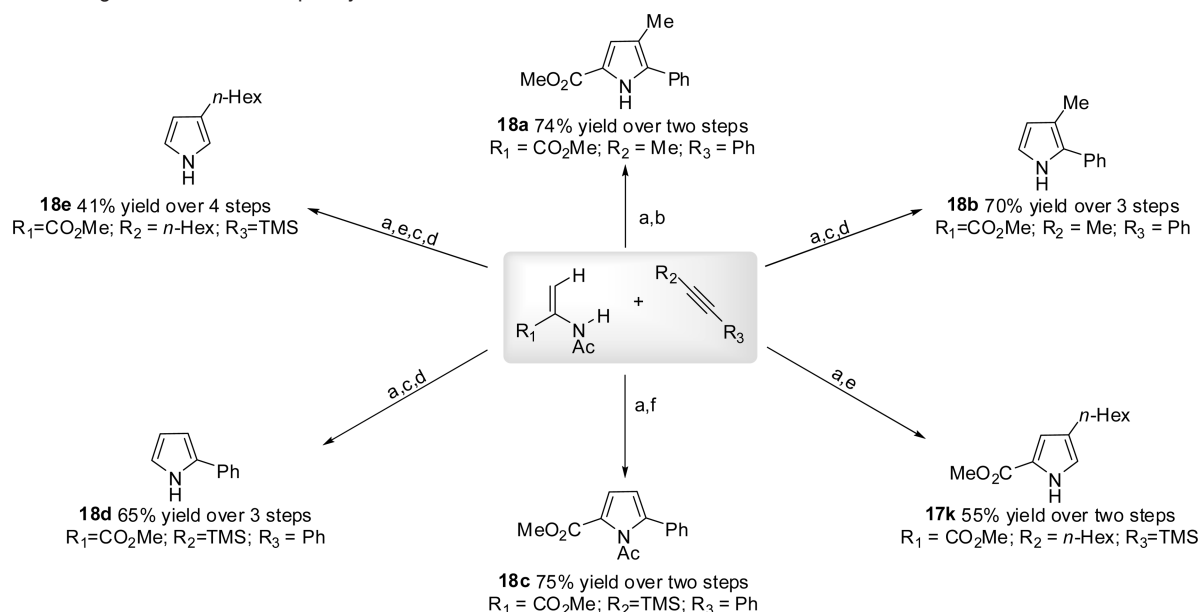
^b Conditions (at 21 °C, blue): as above, in acetone, 21 °C, 16 h. ^c Isolated yields are reported above. ^d See Supporting Information for details of TMS cleavage. ^e 2 equiv of enamide used to 1 equiv of alkyne.

trisubstituted pyrroles with excellent levels of regioselectivity for the aryl group proximal to the pyrrole nitrogen (Chart 3, entries 4–10). Notable among these examples was the variety of functional groups that were tolerated on the alkyl substituent of the alkyne. Pyrroles with a C3 ester (Chart 3, entries 6 and 7), C3 benzyl ester (Chart 3, entry 8), benzyl silyl ether (Chart 3, entries 5 and 9), and benzyl amine protected as a phthalimide (Chart 3, entry 10) were obtained in moderate to good yields under the reaction conditions. While the enamide scope was limited at this stage, initial examples demonstrate that aryl and heteroaryl enamides were also compatible resulting in biaryl and heterobiaryls (Chart 3, entries 13–15); additionally, the use of *N*-vinylacetamide provided direct access to 2,3-substituted pyrroles, albeit in low yield (Chart 3, entry 16). The synthetic utility of the reaction was further qualified by the use of TMS-substituted alkynes, which allowed for the incorporation of a silyl group onto the pyrrole (Chart 3, entry 11 and 12).

Manipulation of these groups, as well as the methyl ester (in compounds **17a–l**), ultimately provided access to a number of other pyrrole substitution patterns (vide infra).²³

Synthetic Applications: Strategies To Access Multiple Pyrrole Substitution Patterns. The high functional group compatibility of the pyrrole forming reaction from enamides and alkynes directly lead to the ability to access a variety of pyrrole substitution patterns. Namely, the incorporation of trimethylsilyl and ester functionality into the alkyne and enamide, respectively, allowed for facile and high yielding removal of these groups after pyrrole formation occurred. Scheme 7 provides conditions for the removal of these groups as well as representative examples of the possible pyrrole substitution patterns that may be obtained.

Removal of the methyl ester in **17a** may be accomplished in high yield (86%) over two steps involving saponification of the ester using LiOH followed by TFA-mediated decarboxylation. This

Scheme 7. Strategies To Access Multiple Pyrrole Substitution Patterns^a

^a Conditions: (a) **2** (5 mol %), Cu(OAc)₂·H₂O (20 mol %), O₂ balloon, acetone, 21 °C, 16 h. (b) 1 N HCl_(aq), THF 60 °C, 17 h. (c) LiOH·H₂O (10 equiv), THF:H₂O (1:1), 60 °C, 17 h. (d) TFA (0.1 M), 0–21 °C, 40 min to overnight. (e) TBAF (1.2 equiv), THF, 21 °C, 18 h. (f) 2 N HCl (in Et₂O), 21 °C, 18 h.

process was used in the formation of pyrroles **18b**, **18d**, and **18e**, and, in all cases, chromatographic purification is only required on the final product. It should also be noted that in these cases under the basic conditions needed for ester saponification, the *N*-acetyl group was also cleaved. The C2-TMS group may be cleaved from the crude pyrrole product by exposure to TBAF (1 M in THF) to yield the C2-unsubstituted pyrrole **17k**. The two-step protocol of oxidative coupling/TMS-cleavage was performed in 55% overall yield (one chromatographic purification) (Scheme 7). These conditions were, however, unsuitable for cleavage of the C3-TMS group of **17l**. In this case, anhydrous HCl (2 N in Et₂O) is necessary and the TMS group was cleaved in near quantitative yield without the need for chromatographic purification, providing pyrrole **18c** (Scheme 7). It should be noted that while exposure to TBAF or aqueous HCl will cleave the *N*-acetyl moiety, anhydrous HCl leaves this group intact, providing orthogonal methods for TMS group cleavage.

Given the operationally simple and high yielding methods outlined above, six of the nine possible pyrrole substitution patterns may be accessed as 2,3,5-, 2,3-, 2,4-, 2,5-, 2-, and 3-substituted pyrroles in good overall yields. Compound **18e** is an interesting example demonstrating the power of this method. Its synthesis has only been reported on one other occasion in the literature and was achieved in five steps in 25% overall yield from a preformed pyrrole.⁴⁵ The inherent challenge in the preparation of this class of compound directly from pyrrole derives from the need to alkylate the least nucleophilic position of the heterocycle. Additionally, the use of primary alkyl halides in Friedel–Crafts chemistry typically suffer from carbocation rearrangements. Thus, this method allows, among other things, the construction of C3-alkylated pyrroles from simple and readily available starting materials in good yield and in an expedient manner.

Conclusion

We have developed a novel and mild method for the construction of highly functionalized indoles and pyrroles based on a rhod-

ium(III)-catalyzed C–H bond functionalization event of arenes and alkenes. The reactions feature good substrate scope with respect to both coupling partners and employ molecular oxygen as the stoichiometric terminal oxidant. A mechanistic investigation of the indole-forming reaction established a viable catalytic cycle that was consistent with the kinetic data obtained and revealed an inhibitory effect at high alkyne concentrations that was largest for alkyl/alkyl-substituted alkynes. Additionally, the regioselectivity of the C–H bond cleavage was found to be dependent on both temperature and alkyne concentration and thus enabled the development of improved conditions for enhanced regioselectivity of meta-substituted acetanilides. The mechanism of the C–H bond cleavage was investigated, and the evidence gathered points toward an irreversible and rate-determining CMD transition state. Finally, the utility of these protocols were demonstrated by the facile and expedient synthesis of paullone, a compound with known bioactivity, and the ease with which a number of pyrrole substitution patterns may be accessed from the cleavage of common functional groups. Given these points, the reactions developed here should find widespread use in synthetic organic chemistry, and the mechanistic insights garnered should aid in the future development of rhodium(III)-catalyzed heterocycle syntheses.

Acknowledgment. We thank NSERC, the Research Corporation, the Sloan Foundation, the ACS (PRF AC), Merck Frosst, Merck Inc., Amgen, Eli Lilly, Astra Zeneca, and Boehringer Ingelheim for financial support. D.R.S. thanks NSERC for a postgraduate scholarship (PGS-D). Professors Tom Rovis, Laurel Schafer, and André Beauchemin are acknowledged for insightful comments and assistance during the preparation of this manuscript. Dr. Benôit Liégault and Sophie Rousseaux are acknowledged for critical reading of the manuscript.

Supporting Information Available: Detailed experimental procedures, characterization data for all new compounds, and complete ref 44. This material is available free of charge via the Internet at <http://pubs.acs.org>.

JA1082624

(45) Reaxys search of compound **18e** provided only one hit: Garrido, D. O. A.; Buldain, G.; Ojea, M. I.; Frydman, B. *J. Org. Chem.* **1988**, *53*, 403.